

Supplementary Information for

Architected van der Waals epitaxy of ZnO nanostructures on hexagonal BN

Hongseok Oh^{1,5}, Young Joon Hong^{2,5}, Kun-Su Kim³, Sangmoon Yoon³, Hyeonjun Baek¹, Seoung-Hun Kang⁴, Young-Kyun Kwon⁴, Miyoung Kim³ & Gyu-Chul Yi¹

¹Department of Physics and Astronomy, Institute of Applied Physics, Seoul National University, Seoul 151-747, Korea.

²Department of Nanotechnology and Advanced Materials Engineering, Graphene Research Institute, and Hybrid Materials Research Center, Sejong University, Seoul 143-747, Korea.

³Department of Materials Science and Engineering, Seoul National University, Seoul 151-747, Korea.

⁴Department of Physics, Research Institute of Basic Science, Kyung Hee University, Seoul 130-701, Korea.

⁵These authors contributed equally to this work.

Correspondence: Professor G-G Yi, Department of Physics and Astronomy, Institute of Applied Physics, Seoul National University, Seoul 151-747, Korea.

E-mail: gcyi@snu.ac.kr

This file includes:

Supplementary Figures and Captions 1–7;

Supplementary References

Supplementary Figures and Captions

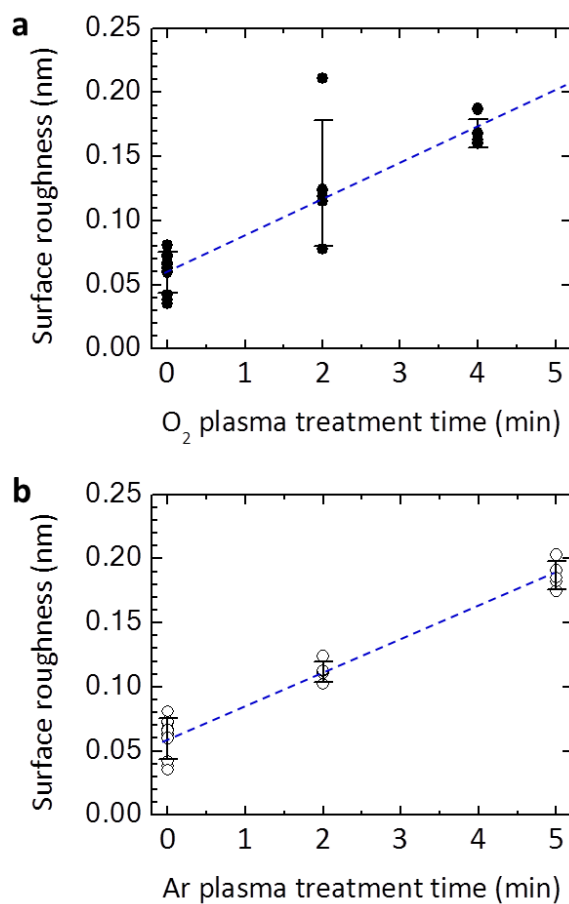


Figure S1 Plots of root-mean-square roughness of the hBN layer treated by (a) oxygen and (b) argon plasma as a function of the plasma treatment time. The roughness was characterized on the step-edge-free hBN areas of $1 \times 1 \mu\text{m}^2$ to clarify the roughening effect of plasma treatment. Error bars denote the standard deviations.

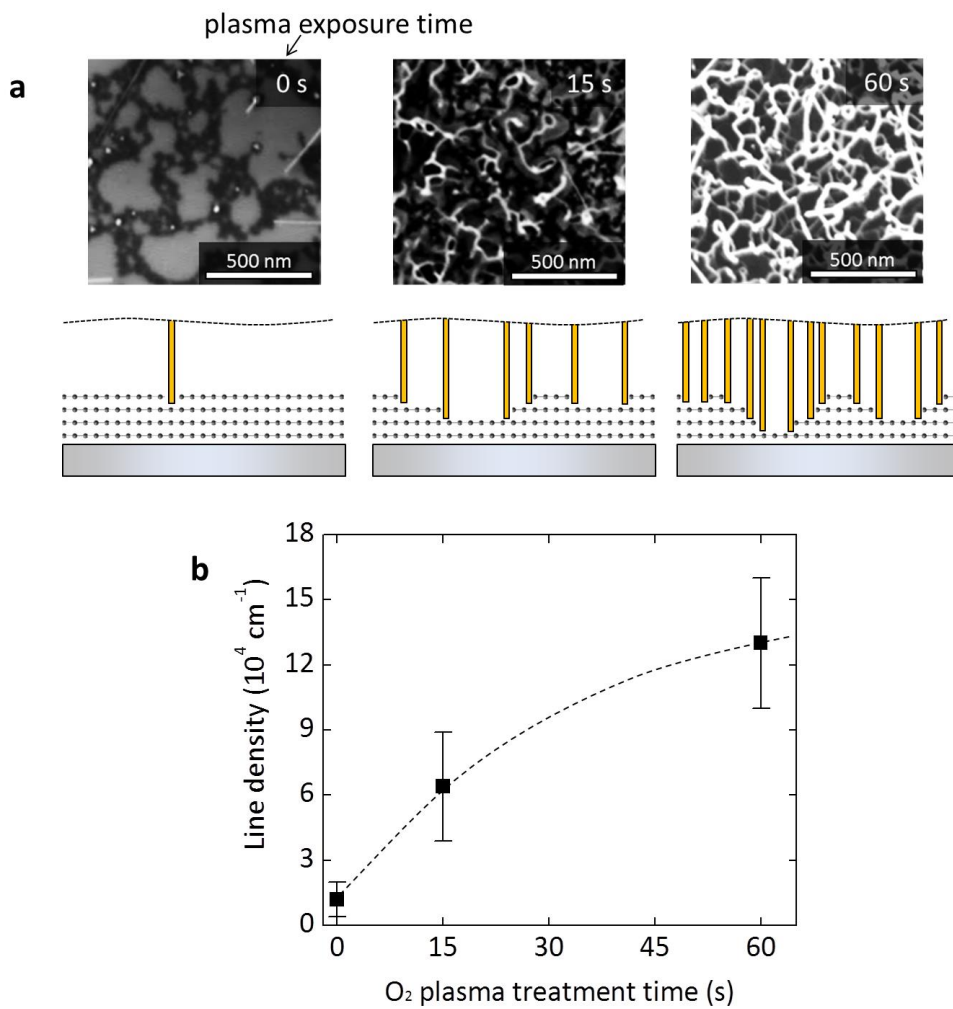


Figure S2 Effect of hBN surface roughness on nanowall density. (a) Top-view SEM images of ZnO nanowalls formed on hBN layers treated by oxygen plasma for 0, 15, and 60 sec. (b) Plot of nanowall line density as a function of the plasma treatment time. Error bars denote the standard deviations.

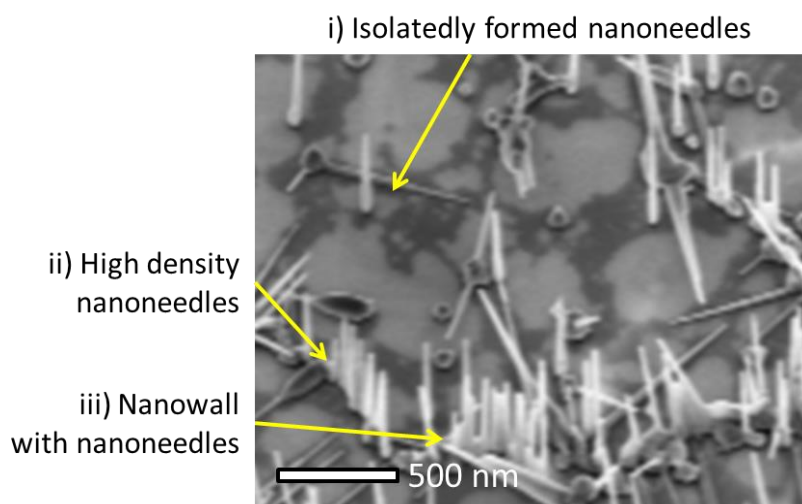


Figure S3 Tilt-view SEM image of ZnO nanostructures grown on bare hBN exfoliated from hBN crystallites. Three different morphologies are obtained: i) isolatedly grown ZnO nanoneedles; ii) high density nanoneedles or iii) nanowall with high density nanoneedles in a specific alignment.

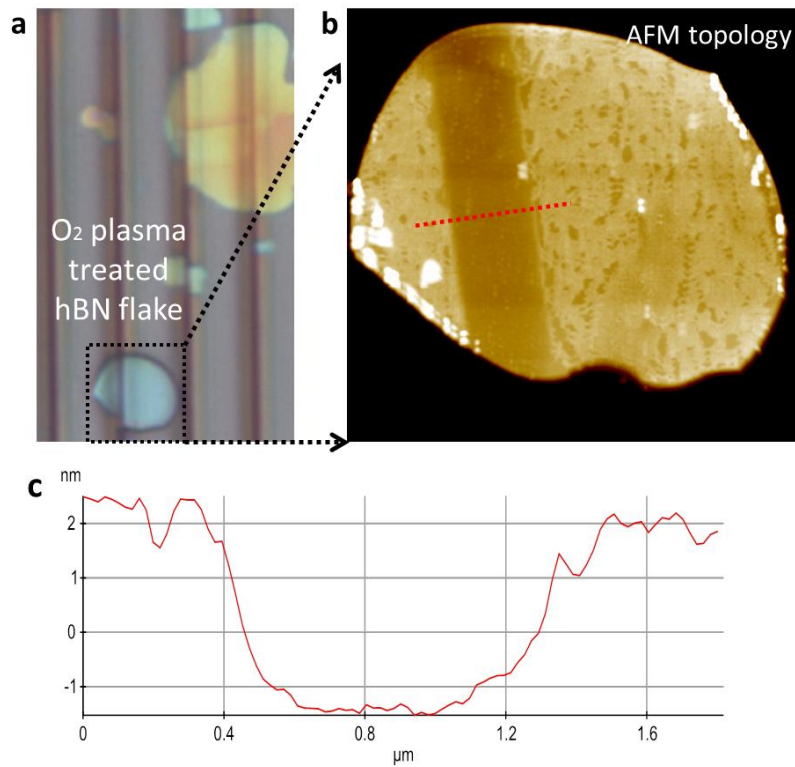


Figure S4 hBN layer etched by plasma treatment. (a) Optical micrograph of hBN layer treated by oxygen plasma for 1 min via polymer resist layer with line-opening patterns. (b) AFM topological map of hBN flake marked in (a). The polymer resist was removed before the AFM measurement. (c) Depth profile of the hBN surface measured along the red dotted line depicted in (b). The etch rate is estimated to be $0.5\text{--}0.8 \text{ \AA sec}^{-1}$.

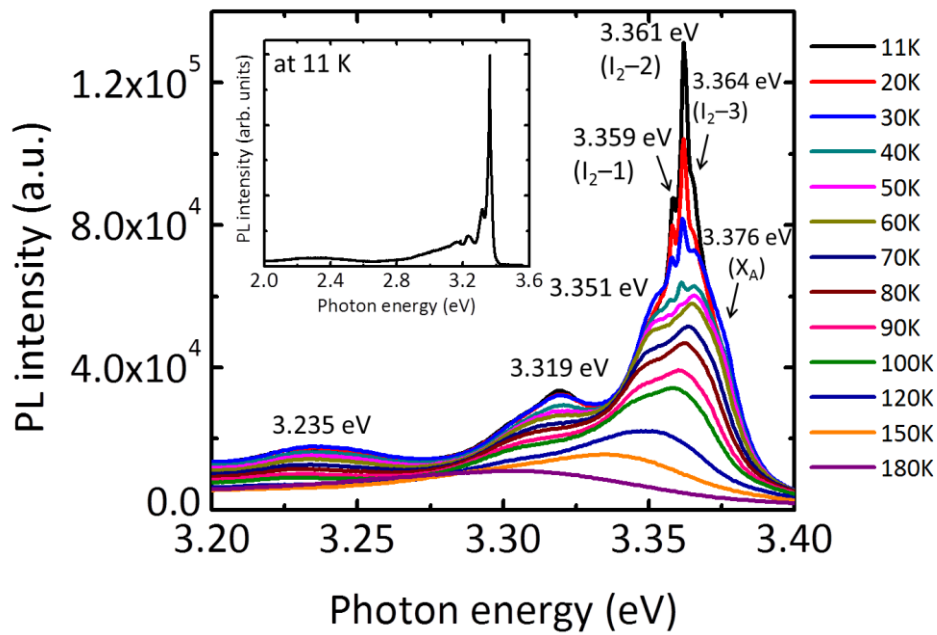


Figure S5 Photoluminescent characteristics of ZnO nanoarchitectures grown on hBN by vdW epitaxy. A series of PL spectra was measured at various temperatures in the range of 11–180 K. The spectrum at 11 K shows seven distinct NBE emission peaks at 3.376, 3.364, 3.361, 3.359, 3.351, 3.319, and 3.235 eV. The PL peak at 3.376 is attributed to a free exciton peak (X_A). The peaks at 3.359, 3.351, and 3.364 eV are ascribed to neutral-donor bound excitonic emissions (I_2) [see Ref. S1, S2]. The sharp and strong NBE emission indicates high optical quality of ZnO nanoarchitectures grown by vdW epitaxy (see inset). The excellent PL properties may result from the high crystallinity of ZnO nanoarchitectures because threading dislocations were not generated from the vdW heterointerface, as confirmed by HRTEM observations.

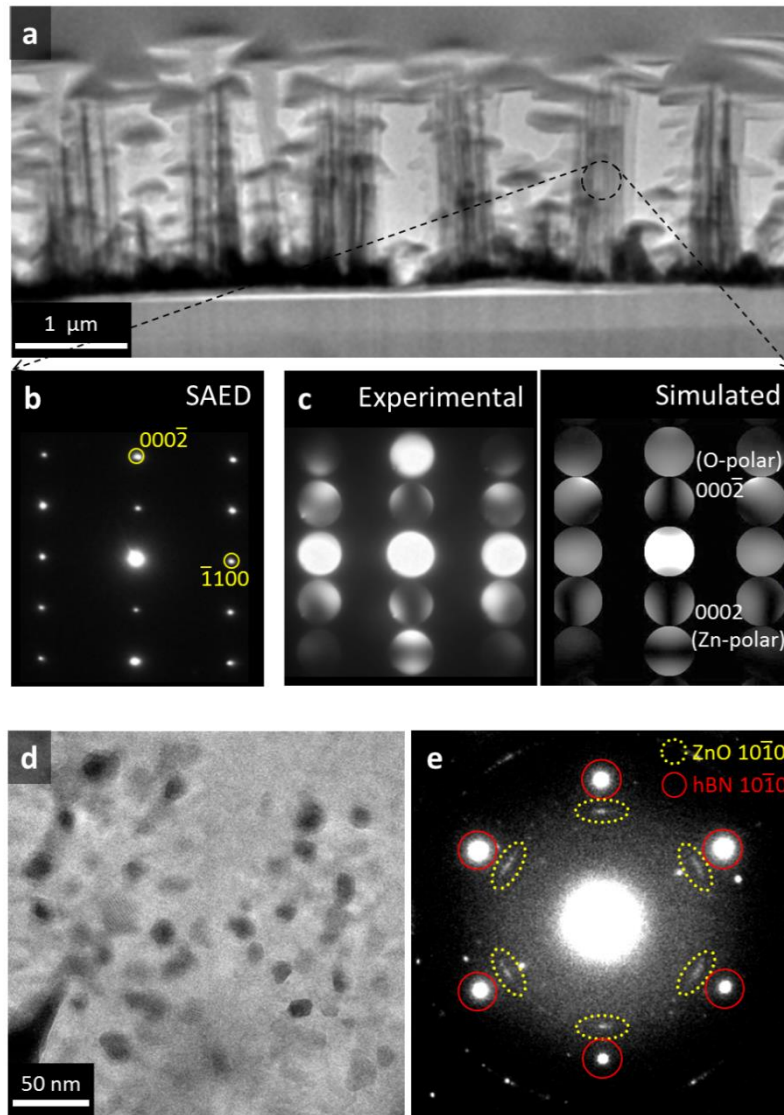


Figure S6 Transmission electron microscopic analysis of ZnO nanoarchitectures. (a) Cross-sectional low-magnification TEM image of ZnO nanostructure arrays. (b) Selected-area electron diffraction (SAED) patterns obtained from the dotted line circle marked in (a), confirming the single crystallinity of the nanoarchitectures. The ZnO nanoarchitectures grew along the c -axis of wurtzite normal to the surface of hBN. (c) Experimental and simulated convergence beam electron diffraction (CBED) patterns of ZnO nanoarchitectures preferentially grown along the O-polar $(000\bar{1})$ direction. The sample thickness for CBED was 37 nm, and the simulation was performed under the same thickness condition. Plan-view (d) low-magnification TEM image and (e) SAED patterns of ZnO nanowalls grown on few-layer hBN. The SAED patterns exhibit the heteroepitaxial relationship of $(000\bar{1})[10\bar{1}0]_{\text{ZnO}} \parallel (000\bar{1})[10\bar{1}0]_{\text{hBN}}$.

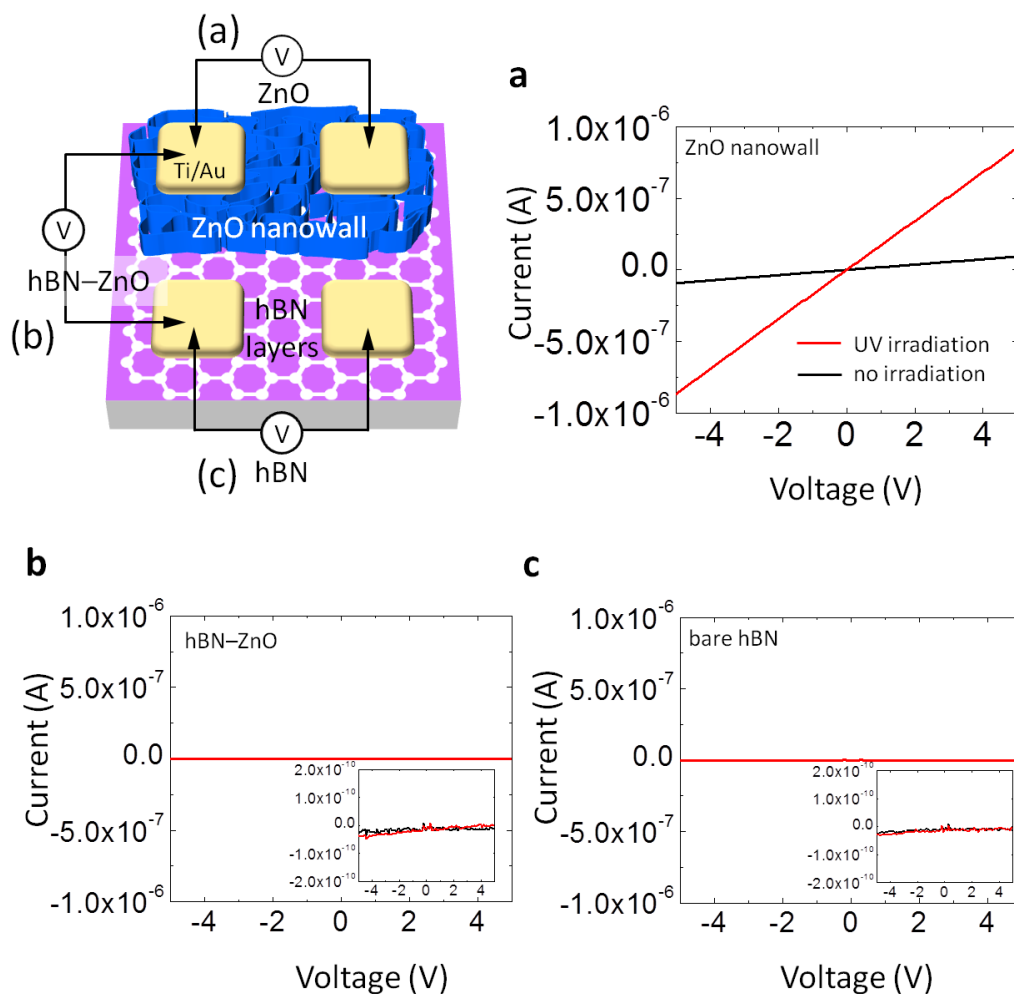


Figure S7 I - V characteristic curves of (a) ZnO nanowalls, (b) ZnO nanowall-hBN heterojunction, and (c) bare hBN layer measured under UV irradiation (red lines) and (black lines) dark room conditions.

Supplementary References

[S1] D. C. Reynolds, D. C. Look, B. Jogai, C. W. Litton, T. C. Collins, W. Harsch, G. Cantwell, *Phys. Rev. B* **1998**, *57*, 12151–12155.

[S2] B. K. Meyer, H. Alves, D. M. Hofmann, W. Kriegseis, D. Forster, F. Bertram, J. Christen, A. Hoffmann, M. Straßburg, M. Dworzak, U. Habocek, A. V. Rodina, *Phys. Status Solidi B* **2004**, *241*, 231–260.